

Mechanisms of Reforming Reactions on Pd/Al₂O₃ Catalysts

F. LE NORMAND,¹ K. KILI,² AND J. L. SCHMITT

Laboratoire de Catalyse et de Chimie des Surfaces, Institut Le Bel, Université Louis Pasteur, 67037 Strasbourg Cedex, France

Received June 3, 1991; revised February 14, 1992

The influence of palladium precursor salt, calcination temperature, and metallic dispersion on the activity and selectivity of reforming reactions on Pd/Al₂O₃ catalysts have been investigated. Reforming reactions involve methylcyclopentane (MCP) hydrogenolysis, 2- and 3-methylpentane (2MP and 3MP) isomerization, dehydrocyclization and hydrocracking, and finally 3-methylhexane (3MH) aromatization. When necessary, ¹³C-labelled hexanes have been used to determine more accurately the selectivity pathways. We find that the mechanistic pathways involve metallacyclic and π olefin- σ alkyl intermediates: metallacyclobutanes and metallacyclopentanes for hydrocracking (essentially demethylation) and bond shift isomerization; 1,2 π -5 σ intermediates for dehydrocyclization, cyclic isomerization, hydrogenolysis of cycles, and hydrocracking of heptanes; and 1,2 π -6 σ intermediates for aromatization. The selectivity obtained in these reactions is discussed in terms of the relative stability of these intermediate species and the kinetic steps of the overall process. The influence of metallic dispersion, palladium precursor salt, and calcination temperature both on the selectivity and the activity is investigated. © 1993 Academic Press, Inc.

INTRODUCTION

Reforming reactions of hydrocarbons including isomerization, dehydrocyclization, aromatization, hydrocracking, and hydrogenolysis of cyclic compounds are well known to occur on platinum catalysts, more often allied with another metal such as Re, Ge, Sn or Ir. Such catalysts have been intensively studied and the influence of preparation parameters (precursor salt, pretreatment, method of preparation, nature of the support, alloying) on the activity and selectivity has long been recognized (1). Thus the effect of metallic dispersion, surface morphology of the particles, and interaction with the support on the mechanistic pathways of hydrocarbons is outlined (2, 3).

However, platinum is expensive and scarce, so that there is a need to substitute for it.

Palladium is a possible candidate for this substitution, as it has been known for a long time to exhibit activity in all the above-mentioned reactions (4, 5). The use of labeled hydrocarbons by the Gault group allowed us to recognize the main mechanistic pathways on palladium. Thus Hajek *et al.* (6) showed that the main isomerization mechanism of hexanes occurs through an adsorbed methylcyclopentane intermediate (cyclic mechanism), whereas a small but definite contribution could be attributed to a bond shift mechanism. Aromatization of (¹³C) 3-methylhexane occurs through a main direct 1-6 cyclization instead of the indirect 1-5 cyclization (7, 8). Hydrocracking has been studied by the group of Paál and Tétényi (8). The main reaction is a single demethylation on the less-substituted carbons. However, mechanistic studies have been performed on catalysts with large particles only (6, 7). Moreover, in contrast to platinum catalysts, only a few studies have been devoted to the influence of preparation and pretreatments

¹ To whom correspondence should be addressed. Present address: Institut de Physique et Chimie des Matériaux (IPCMS), Groupe Surfaces-Interfaces, Institut Le Bel, Université Louis Pasteur, 4 rue Blaise Pascal, 67070 Strasbourg Cedex, France.

² Present address: Faculté des Sciences, Université du Bénin, BP 1515, Lomé, Togo.

on the reforming activity and selectivity of palladium catalysts. Palladium films deposited on various supports emphasize the influence of surface morphology in neopentane isomerization as a test reaction (9). Several more recent works underline the influence of support and catalyst pretreatments on neopentane reactivity (10–12). Activity in cyclopentane hydrogenolysis remains insensitive to the metallic particle size (13). Other works have been devoted to alloying effects, by an inactive diluent such as Ag (14) or Au (15, 16) or by an active diluent such as Rh (17).

The aim of this work is to obtain further improvements on knowledge of the mechanisms encountered on palladium in reforming reactions and to investigate the influence of some preparation parameters (temperature of calcination treatment, impregnation method, palladium precursor salt) on the catalytic activity and selectivity. Test reactions include methylcyclopentane (MCP) hydrogenolysis, 2- and 3-methylpentane (2MP and 3MP) isomerization, and 3-methylhexane (3MH) aromatization. When necessary, ¹³C-labelled hydrocarbons were used to specify more accurately the mechanistic pathway. Characterization studies include TEM and XPS.

METHODS

1. Catalyst Preparation

(a) *Support.* The support is γ -Al₂O₃ Woelm (BET surface area 160 m²/g, pore volume 0.28 cm³/g, mean pore diameter 3.4 nm).

(b) *Precursor salt.* The following precursor salts were used:

—Palladium acetylacetonate, Pd (acac)₂ (Series I).

—Palladium dinitrate, Pd (NO₃)₂ (Series III).

—Palladium dichloride tetrammine, Pd (NH₃)₄ Cl₂ (Series IV, V, VI, and VII).

All products were provided by Johnson Matthey (purity 4 N). In addition, we tested

a catalyst furnished by the Institut Français du Pétrole (I.F.P.) (Series II).

(c) *Impregnation.* Catalysts were generally prepared by the classical dry impregnation of the γ -Al₂O₃ support of a required amount of an aqueous solution of palladium salt [Pd(NH₃)₄Cl₂ or Pd(NO₃)₂]. Powders were then dried in an oven at 120°C for 24 h. Catalysts of Series I were prepared by impregnation of palladium acetylacetonate diluted in a benzene solution according to Boitiaux *et al.* (18). After evaporation of the solvent, the powder was dried in an oven at 120°C. Catalysts of Series IV were prepared by cation exchange of a 10⁻¹ N aqueous solution of Pd(NH₃)₄Cl₂ at pH = 10 for 24 h at room temperature. The metallic concentration in solution was followed by atomic absorption spectroscopy.

After drying, the metallic loading was determined by microanalysis performed at the Service Central de Microanalyse du CNRS (Vernaison, France) (see Table 1).

2. Catalytic Tests

(a) *Treatments.* Treatments of catalysts of Series I to IV were performed in an all-glass, grease-free, and atmospheric pressure reactor already described (19). Unless otherwise stated, catalysts were treated by a precalcination under synthetic air at a given temperature for 4 h. The increase in temperature was 2°C/min and the gas flow was 20 ml/min. The temperature was then decreased to 25°C and the catalyst was flushed with nitrogen for half an hour; hydrogen was admitted and the reduction was then carried out. The temperature was increased up to the reduction temperature (2°C/min, 20 ml/min) followed by 1 h at 300°C. Calcination and reduction temperatures are given in Table 1.

Catalysts of Series VI were initially calcined in an oven able to provide high-temperature treatments. The container was a ceramic crucible. After flushing with nitrogen, samples were stored in a desiccator before further use. Reduction conditions

TABLE I
Characterization Properties of Pd/ γ -Al₂O₃ Catalysts

Catalyst	Pd (wt%)	Palladium precursor salt	Treatment temperature (°C)		TEM <i>d</i> _v (nm)
			Calcination	Reduction	
I-1	0.8	Pd(acac) ₂	300	300	2.5
II-1 ^b	0.45	Pd(acac) ₂	—	300	—
II-2 ^b	0.45	Pd(acac) ₂	300	300	1.5 ^b
III-1	0.75	Pd(NO ₃) ₂	200	400	8.2
IV-1 ^a	0.33	Pd(NH ₃) ₄ Cl ₂	400 ^c	400	—
V-1	1.1	Pd(NH ₃) ₄ Cl ₂	200	400	3.5
VI-1	9.3	Pd(NH ₃) ₄ Cl ₂	—	400	12.0
VI-2	9.3	Pd(NH ₃) ₄ Cl ₂	200	400	—
VI-3	9.3	Pd(NH ₃) ₄ Cl ₂	400	400	5.7
VI-4	9.3	Pd(NH ₃) ₄ Cl ₂	600	400	6.1
VI-5	9.3	Pd(NH ₃) ₄ Cl ₂	770	400	>10
VI-6	7.5	Pd(NH ₃) ₄ Cl ₂	900	400	12
VI-7	9.3	Pd(NH ₃) ₄ Cl ₂	400	300	—
VII-1	0.04	Pd(NH ₃) ₄ Cl ₂	200	400	—

^a Prepared by ion exchange.

^b I.F.P. catalyst.

^c Calcination 10 h.

were the same as described above. Surface areas fell from 130 to 90 m²/g after the calcination at 900°C.

(b) *Catalytic tests.* Catalytic tests were performed under 1 atm H₂ pressure by pulse of hydrocarbon at constant hydrocarbon pressures which were 4, 6, 6, and 5 Torr for the MCP, 2MP, 3MP, and 3MH reagents, respectively. Before any activity and selectivity measurements, the catalyst was preliminarily saturated by some hydrocarbon pulses until a quasi-stability in the catalytic activity and selectivity was observed. It was checked that the deactivation rate was still negligible. Reaction temperature was 300°C for methylcyclopentane, 2- and 3-methylpentane and 360°C for 3-methylhexane.

Reagents were Fluka puriss grade. They contained some impurities whose amounts were frequently checked by on-line analysis before the reactor. Impurity levels were 0.6 ± 0.2% of *n*-hexane and cyclohexane in MCP, 0.1% of 3-methylpentane in 2MP, and 1.0% of 2-methylhexane plus 2,3-dimethylpentane and 2.7% of *n*-heptane for 3MH. These impurities were subtracted in the product analysis.

Products of MCP and 2MP were analyzed on a chromatographic column of silicone oil DC200 at 5% on firebrick. In 2MP isomerization, 2,3-dimethylbutane was separated from cyclopentane only by mass spectrometry coupled with gas chromatography (MS-GC).

3MH products were analyzed on a capillary silicone column OV101. In the conditions of use, the following hydrocarbons could not be separated in the M3H analysis: (a) 2-methylhexane and 2,3-dimethylpentane, (b) methylcyclohexane and *cis*-1,2-dimethylcyclopentane. We assumed a ratio for *trans/cis* 1,2-dimethylcyclopentane of 4, as determined in a previous study (7) by MS-GC.

After reaction, the reactor was cooled down to room temperature and the catalyst was passivated by slow admission of nitrogen.

(c) *Labelled experiments.* The complete process of synthesis and purification of the ¹³C-labelled hydrocarbons as well as the determination of the ¹³C label in the isomerization products of hexanes was described elsewhere (20).

(d) *Kinetic studies.* Kinetic studies were carried out in a small temperature range where a low level of conversion could be achieved. Activation energies were determined both in the increasing and decreasing temperature mode.

In the limit of a low conversion level α_T , the overall activity A_T in $\mu\text{mol/s} \cdot \text{g}_{\text{Pd}}$ can be defined according to

$$A_T = \alpha_T \cdot F/\omega, \quad (1)$$

where F is the hydrocarbon flux (in $\mu\text{mol/s}$) and ω the weight of palladium (g_{Pd}). We checked that in our experimental conditions no diffusional limitations impeded the catalytic activity and the initial product distribution measurements.

3. Transmission Electron Microscopy (TEM)

Catalysts were examined after catalytic use on a Philips EM300G transmission electron microscope (Laboratoire de Cristallographie de l'Université Louis Pasteur, Strasbourg, France). The accelerating voltage was 100 kV. The optical magnification was 320,000. The extractive replica technique was used (21). Catalysts were treated for 1 h in 10% HF solution to dissolve the support. Microdiffractions on selective areas were carried out to check that only palladium particles were present. It was checked that no sintering of the palladium particles occurred with a time of HF treatment up to 20 h.

The mean size of the crystallites \bar{d}_v from the ratio volume to surface distribution (22–24) was determined as

$$\bar{d}_v = \frac{\sum n_i \cdot d_i^3}{\sum n_i \cdot d_i^2}, \quad (2)$$

where n_i is the amount of counted particles (overall about 2000) of mean diameter d_i .

4. Photoemission Studies (XPS)

The apparatus, sample preparation, data collection, lineshape, and surface content analysis were presented elsewhere (26).

RESULTS

1. TEM

Results are summarized in Table 1. The histograms of the particle distribution of catalysts I-1 and VI-3 are depicted in Fig. 1b. A satisfactory homogeneity and dispersion of particles are observed on the catalysts obtained from the acetylacetonate precursor. The mean diameter according to Eq. (2), however, gives an overestimate, as the particles of size less than 0.5 nm cannot be counted. As we measured by H₂ chemisorption a metallic dispersion of 58% on this catalyst (25), we can estimate the lower and the upper limits of the mean particle size to be 1.5 and 3.0 nm, respectively. In the other cases, larger particles coexist with smaller particles, resulting in some heterogeneity in the histogram (Fig. 1b). Mean particle sizes from ca. 3.5 nm to more than 10 nm were then measured, but these values must only be considered as indicative. On these catalysts, however, the amount of particles of size less than 2.0 nm is always small or negligible.

2. Methylcyclopentane Hydrogenolysis

At 300°C under a hydrogen pressure of one atmosphere, the carbon-carbon bond rupture results in four products (Scheme 1):

—endocyclic ruptures resulting in *n*-hexane, 2- and 3-methylpentane formation (pathways 1, 2, and 3, respectively), which are reversible reactions in our experimental conditions.

—an exocyclic rupture resulting in cyclopentane (CP) formation (pathway 4), which is then an irreversible reaction.

Up to very high conversion levels, other reactions (1-6 cyclization and multiple carbon-carbon rupture) are generally negligible and always inferior to 3% of the products. We determined in every case the initial distribution by extrapolating the product distribution to zero conversion, as illustrated in Fig. 2 with catalyst V-1. Errors in

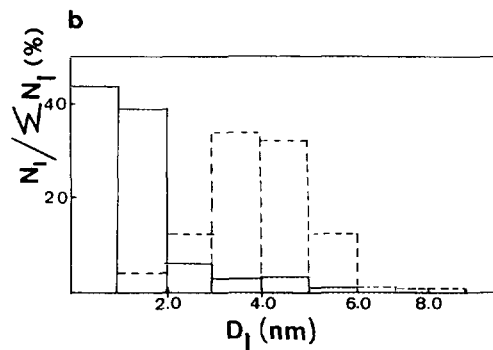
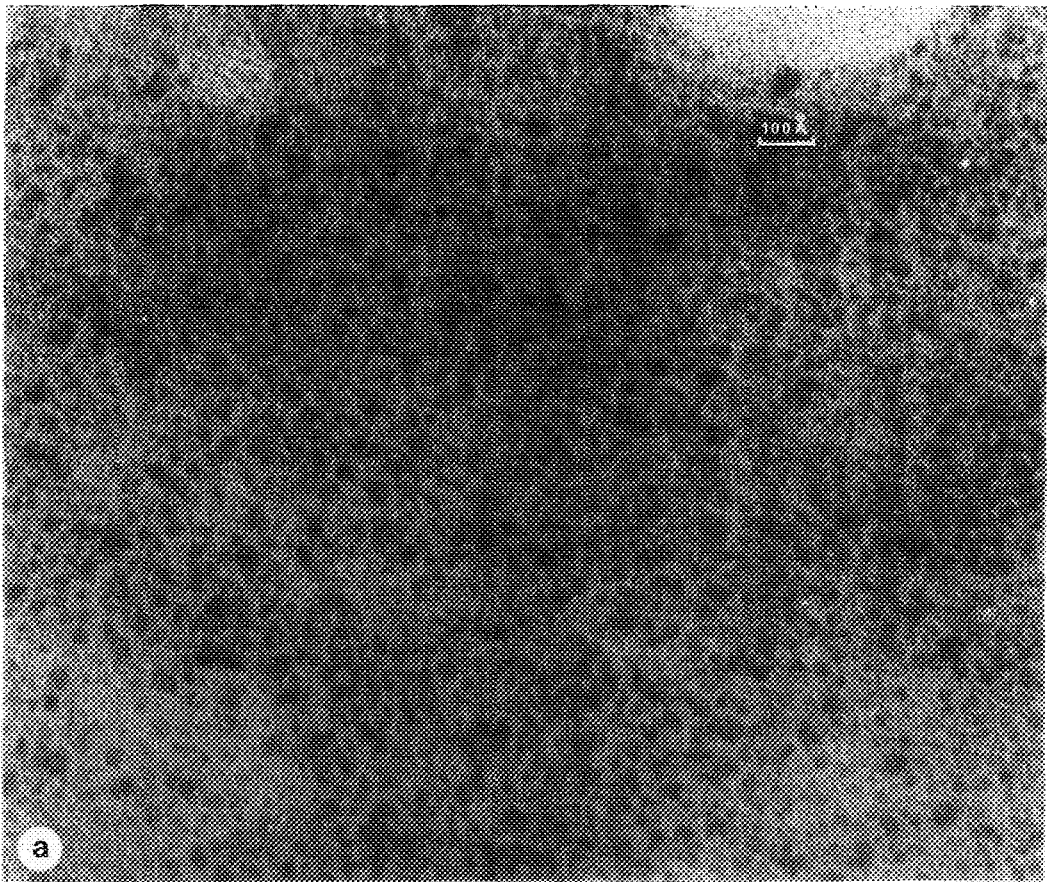
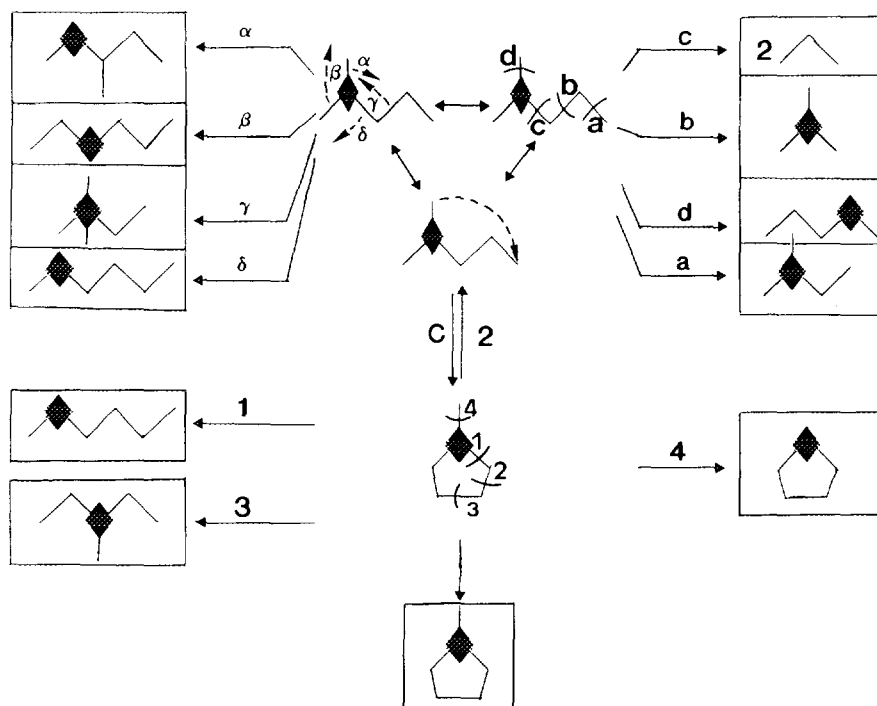


FIG. 1. (a) TEM of samples I-1 (Magnification: 3×10^5) and (b) histogram of the particle size distribution: sample I-1 (full line) and VI-3 (dotted line).

the initial product distribution are estimated to $\pm 2\%$.

Activity and selectivity results are summarized in Table 2. For catalysts with a comparable low palladium loading (Series I

to V) and reduced at the same temperature (400°C), the activity in hydrogenolysis changes over a wide range: the nitrate precursor catalyst is ca. two orders of magnitude less active than the acetylacetonate



SCHEME 1

precursor catalyst or the catalyst prepared by ion exchange, while the chloride precursor catalyst exhibits an intermediate activ-

ity. The influence of the calcination temperature has been studied on the catalysts of the Series VI. The activity decreases slowly with increasing temperature from 200 to 900°C (Fig. 3), but the amplitude of the vari-

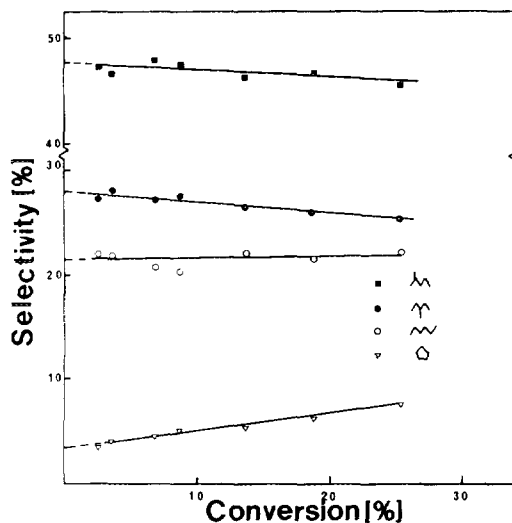


FIG. 2. Methylcyclopentane hydrogenolysis: Plot of the product distribution versus conversion on catalyst V-1 (300°C): CP (∇), 2MP (\blacksquare), 3MP (\bullet), and *n*H (\circ).

TABLE 2

Activity and Initial Product Distribution in MCP Hydrogenolysis on Different Pd/ γ -Al₂O₃ Catalysts ($T = 300^\circ\text{C}$, $P(\text{MCP}) = 4$ Torr, $P(\text{H}_2) = 755$ Torr)

Catalyst	$A_{\text{H}_2, \text{d}}$ ($\mu\text{mol/s} \times \text{g}_{\text{Pd}}$)	Initial distribution (%)			
		CP	2MP	3MP	<i>n</i> H
I-1	110	4	45.5	27	23.5
II-1	30	2	49	26	23
II-2	83	4	45.5	27	23.5
III-1	0.6	4	54	24	18
IV-1	90	4	42	32	21
V-1	34	3	48	28	21
VI-3	2.9	4	46	25.5	24.5
VI-7	0.16	4	46	25.5	24.5
VII-1	84	4	46	27	23
Distribution (A)	—	—	40	20	40
Distribution (B)	—	—	33	33	33
Distribution (C)	—	—	50	25	25
Thermodynamic equilibrium (Ref. (27))	—	—	45	25	30

ation does not exceed one order of magnitude. This effect is also apparent with the acetylacetonate precursor catalysts (catalysts II-1 and II-2).

The influence of the reduction temperature is also strong. When reduction is carried out at 300 instead of 400°C, we note a

large decrease as we compare the activity of catalysts VI-3 and VI-7, respectively.

Whatever the treatments given to the catalyst, there is only little change in the initial product distribution. The hydrogenolysis products rank in the following decreasing order:

$$\begin{array}{l} \text{2MP} \gg \text{3MP} > n\text{H} \gg \text{CP} \\ \text{initial distribution (\%)} \quad (42-49) \gg (25-28) > (21-24) \gg (2-4). \end{array}$$

We note that only the nitrate precursor catalyst (III-1) behaves differently from the other Pd/ γ -Al₂O₃ catalysts as the probability of formation of 2-methylpentane is slightly enhanced at the expense of 3MP and *n*-hexane.

Comparing furthermore with the statistical carbon-carbon bond probability of rupture, namely, $(\lambda_{\text{stat}})_{2\text{MP}}$ for 2MP, we can de-

fine in a way analogous to Leclercq *et al.* (28) the actual probability factor of carbon-carbon bond rupture ω . This probability factor for 2MP takes the form

$$\omega_{2\text{MP}} = \lambda_{2\text{MP}} / (\lambda_{\text{stat}})_{2\text{MP}}, \quad (3)$$

where $\lambda_{2\text{MP}}$ is the initial experimental selectivity. Experimental values of ω rank in the following decreasing order:

$$\begin{array}{l} \text{3MP} > \text{2MP} \gg n\text{H} > \text{CP} \\ \omega \quad (1.25-1.55) > (1.10-1.20) \gg (0.45-0.6) > (0.15-0.4). \end{array}$$

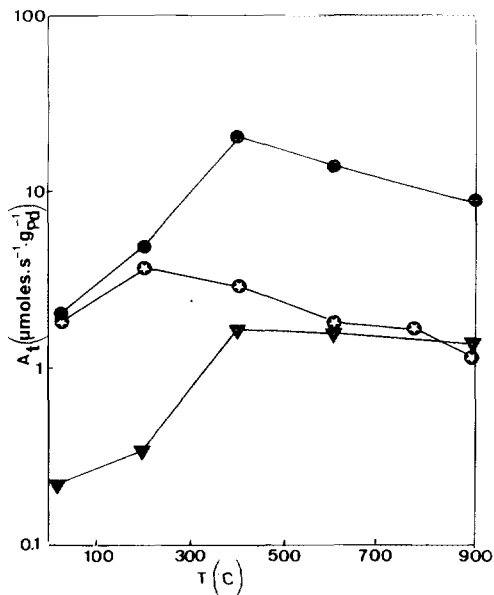


FIG. 3. MCP hydrogenolysis (●), 3MH overall (○), and aromatization (▼) activity as a function of the calcination temperature on Pd/Al₂O₃ catalysts (Series VI).

We can thus note that the carbon-carbon bond rupture probability is larger than the statistical probability when the carbons directly involved in the bond rupture are not substituted by the methyl group (pathways 2 and 3 in Scheme 1).

Activation energies for some Pd/ γ -Al₂O₃ catalysts are given in Table 3 for each carbon-carbon rupture bond. They are determined in a short temperature range around 300°C. Some of them are represented in an Arrhenius plot in Fig. 4. They range between 55 and 65 kcal/mol, without detectable change with the nature of the endocyclic carbon-carbon bond rupture.

(a) *Unlabelled experiments.* At 300°C with palladium, 2-methylpentane can give the following reactions according to Scheme 1.

—Hydrocracking (carbon-carbon bond rupture a to d). Extensive hydrocracking

TABLE 3

Activation Energies in Methylcyclopentane Hydrogenolysis on Pd/Al₂O₃ Catalysts (Errors Are Estimated to ± 3 kcal/mol)

Catalyst	T range (°C)	E _A (kcal/mol)			
		2MP	3MP	nH	CP
I-1	270–300	65	64	64	65
IV-1	270–300	61	60	58	65
VI-3	280–325	57	58	57	62

which gives directly methane and ethane is generally negligible at small conversions.

—Isomerization according to a 1–2 bond shift mechanism (methyl, methyl, ethyl, and propyl shifts for α , β , γ , and δ rearrangement, respectively). All these bond shifts were clearly identified by the use of the ¹³C label (2, 3).

—Dehydrocyclization (C) followed by hydrogenolysis according to the well-known cyclic isomerization mechanism.

Activities in 2MP isomerization are generally one order of magnitude less than MCP hydrogenolysis activities (Table 4). We note especially the low activity of the nitrate precursor catalyst.

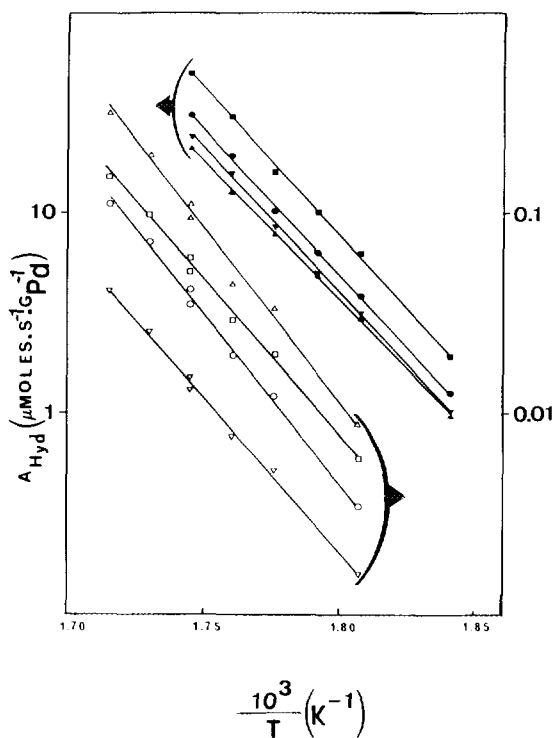


FIG. 4. Arrhenius plot in methylcyclopentane hydrogenolysis on Pd/Al₂O₃ catalysts. Samples I-1 (black dots) and VI-2 (white dots), respectively: (■, □) 2MP; (●, ○) 3MP; (▼, ▽) nH; (▲, △) CP. The rate constants for the CP data are multiplied by 10 before plotting in the figure.

TABLE 4

Isomerization and Hydrocracking of 2-Methylpentane on Pd/Al₂O₃ Catalysts
(T = 300°C; P(2MP) = 6 Torr; P(H₂) = 754 Torr)

Catalyst	A _T [μmol s ⁻¹ g _{Pd} ⁻¹]	α _T (%)	S _{ID} (%)	S _{HC} (%)	2C ₃ (%)	C ₄ + C ₂ (%)	C ₅ + C ₁ (%)	2,2 DMB ^a (%)	3MP (%)	nH (%)	MCP (%)
I-1	9.8	2.0	71	29	2	4	23	tr ^b	11	13	47
II-2	22	3.9	60	40	2	3	35	tr	14	12	34
III-1	0.1	0.13	50	50	8	2	40	—	5	4	41
IV-1	15	3.3	54	46	1	2	43	1	17	12	25
VI-1	—	5.8	41	59	1	2	56	2	11	8	20
VI-2	—	11	55	45	2	3	49	1	15	13	16
VI-3	—	8.0	58	42	1	2	38	tr	16	11	30
VI-5	—	11	43	57	2	2	53	tr	16	13	14
VII-1	9.6	8.5	64	36	2	2	32	1	11	9	43

^a 2,2 DMB = 2,2-dimethylbutane.

^b tr = trace.

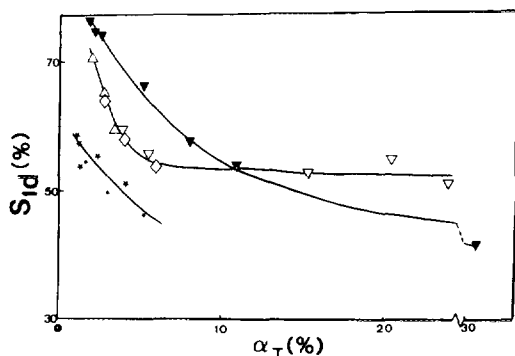


Fig. 5. 2-methylpentane selectivity in isomerization + dehydrocyclization S_{ID} . Evolution with conversion on sample I-1 (\diamond), II-1 (∇), II-2 (\triangle), IV-1 (\star, \ast), and VI-3 (\blacktriangledown).

With unlabelled 2-methylpentane we could determine the selectivity in hydrocracking (S_{HC}) and isomerization plus dehydrocyclization (S_{ID}) products (Table 4). It seems however difficult to establish a general statement concerning the isomerization mechanisms from the sole use of unlabelled methylpentane for two reasons at least. First we cannot discriminate between isomers (3MP and n H) formed according to the bond shift or the cyclic mechanism (Scheme 1). We note, however, that the relative proportions of 3MP and n H are identical in both MCP hydrogenolysis and 2MP isomerization. Second, the rate of 2MP isomerization being much lower than the rate of MCP hydrogenolysis (compare activities in Tables 2

and 4, respectively), consecutive reactions may hide the initial product distribution (2). This is clearly seen in Fig. 5, where the selectivity S_{ID} decreases sharply with conversion and is strongly different from the initial product distribution even at moderate conversion. Figure 5 points out also that the selectivity is dependent on the palladium precursor salt and the mode of impregnation. For example, although they exhibit comparable overall activities, the palladium coming from an acetylacetonate precursor salt (Series I and II) gives a higher selectivity S_{ID} than palladium prepared by the ion exchange of a chloride precursor. With catalysts I and II the higher selectivity S_{ID} at high conversion could be explained by the inhibition of consecutive reactions leading to hydrocracking on the smaller particles.

Concerning the hydrocracking pathways, however, some clear points appear. The most intense hydrocracking is demethylation. Among the demethylation products, the rupture a of the primary-secondary carbon bond giving isopentane is promoted over the rupture d of the primary-tertiary carbon bond giving n -pentane (Scheme 1). Using the same parameter ω defined above for methylcyclopentane hydrogenolysis and assuming that consecutive reactions are negligible, which is checked by the high ratio of isobutane (direct) to n -butane (consecutive) formation (20), the probability of carbon-carbon bond rupture on the catalyst II-2 ranges in the following decreasing order:

carbon-carbon bond rupture
(see Scheme 1)
 ω

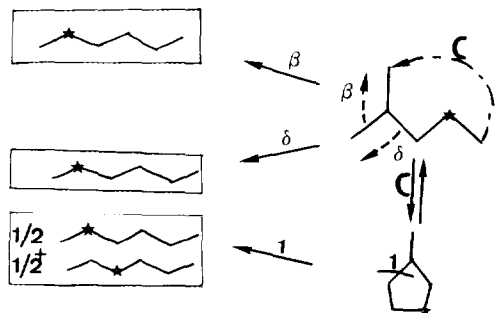
$a > d \gg b > c$
1.54 1.23 0.55 0.42.

These values are only slightly modified with the palladium precursor salt and calcination. They are in agreement with previous reported results (8).

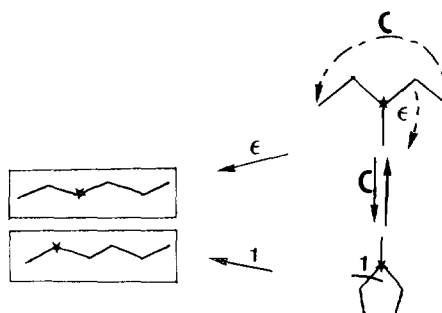
A kinetic study was performed on catalyst VII-1 only. The activation energy for both isomerization and dehydrocyclization is about 57 kcal/mol, a value similar to the

MCP hydrogenolysis activation energies. Activation energies for hydrocracking pathways range from 71 (n -pentane), 67 (isopentane), 50 (isobutane) to 32 kcal/mol (n -propane). Activation energies and frequency factors fit a compensation curve.

(b) *Labelled experiments.* We used three labelled 2- and 3-methylpentanes and the



SCHEME 2



SCHEME 3

analysis of the label in the resulting products allows us to differentiate without ambiguity between the different isomerization pathways and thus to obtain a complete overview on the mechanistic process (Schemes 1, 2, and 3). For example, *n*-hexane can be obtained by three different ways, namely, the bond shifts β and δ and the cyclic mechanism C, whose contributions can be fully determined by the use of 2- and 4-¹³C 2MP reagents (Schemes 1 and 2, respectively). 3-¹³C 3MP allows us to discriminate between the contribution of an ethyl shift ϵ or the cyclic mechanism C in *n*-hexane formation (Scheme 3).

The influences of size effect and palladium precursor salt have been investigated. Focussing on the distribution of the hexanes, we point out that the relative contribution of each isomerization pathway remains

unchanged on widely different dispersions (Table 5). The major labelled products are obtained through an adsorbed methylcyclopentane (Pathway C in Scheme 1) whatever the dispersion or the precursor salt. In every case, products achieved by a direct pathway are obtained with more than 97% selectivity. This indicates a low level of consecutive reactions.

However, we can note some significant mechanistic changes if we deal now with a complete balance of product distribution including the sum of hydrocracking products (HC), isomers produced by the bond shift mechanism (BS), isomers, and MCP produced by the cyclic mechanism (MC) (Table 5). They are compared with two distributions obtained on a 10% Pd (ex chloride)/ γ -Al₂O₃ calcined at 770°C (29) and a 1% Pd (ex chloride)/ γ -Al₂O₃ prepared by

TABLE 5

Isotopic Distribution in 2- and 3-Methylpentane Isomerization. Selectivity According to the Different Pathways

Catalyst	α (%)												HC	BS	CM	
I-J	15	9)	9	0	0	95	5	0	56	44	0	92	8	44	3	53
VI-1	9	71	29	0	0	89	11	0	64	36	0	59	41	62	3	35
VII-1	8	71	29	0	0	91	9	0	59	41	—	—	—	34	7	59
Ref. (29)														58	7	35
Ref. (30) ^a														62	3	35

^a *T* = 330°C.

the precipitation of a microemulsion, a catalyst which exhibits a homogeneous size of particles around 6 nm (30). The following trends appear:

(i) Isomerization according to a bond shift mechanism is always a minor pathway (less than 10%).

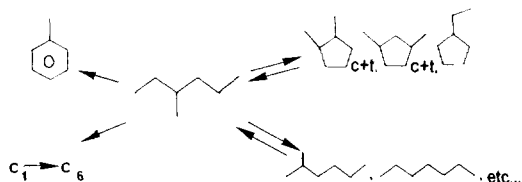
(ii) Isomerization according to a cyclic mechanism is about 35% on catalysts with rather large palladium particle size, ranging from 5 to more than 10 nm. When the palladium phase is well dispersed, however, (catalysts I-1 and VII-1), an increase in the cyclic mechanism to the detriment of hydrocracking can be noted. On the former catalyst the conversion is somewhat high, but we see above (Fig. 5) that the selectivity S_{ID} decreases slowly at conversions higher than 10%. We can estimate to about 20% the increase in the cyclic pathway as the dispersion increases. Moreover, a careful examination of the product distribution in Table 4 outlines a correlation between the increase in the cyclic mechanism and a high proportion of MCP in the product distribution (catalysts I-1, VI-1 and VII-1, respectively).

Finally, the influence of palladium precursor salt on mechanistic pathways is small and probably not significant here, owing to the experimental uncertainty on the label localization and the different conversion level.

4. 3-Methylhexane Aromatization

According to Scheme 4, 3-methylhexane (3MH) can give hydrocracking, isomerization, and 1-5 dehydrocyclization reactions to which must be added aromatization and 1-6 dehydrocyclization reactions.

The influence of metallic dispersion and



SCHEME 4

TABLE 6
3-Methylhexane Aromatization at 360°C on Pd/Al₂O₃
Catalysts (Initial Distribution)

Catalyst	S_H	S_{I+D}	S_A
VI-1	65	27	8
VI-3	59	33	8
VI-6	34	52	14
VII-1	36	57	7

calcination treatments on the overall and aromatization activities and selectivities is reported in Table 6.

As for 2MP, the 3MH selectivities are strongly dependent on the total conversion, so that only the initial distributions must be considered (Fig. 6). On the catalysts of Series VI, the overall activity is maximum after a calcination at 200°C, whereas the aromatization activity reaches a constant level at calcination temperature higher than 400°C (Fig. 3). A decrease in hydrocracking selectivity is obtained by increasing the calcination temperature or the metallic dispersion (Table 6). By calcination, isomerization, dehydrocyclization and aromatization selectivities are noticeably increased, whereas by increasing the metallic dispersion, aromatization selectivity remains unchanged.

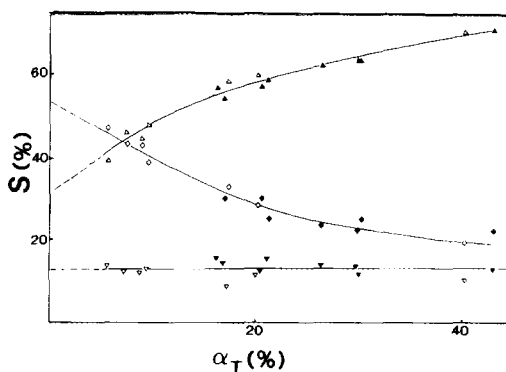


FIG. 6. 3-MH selectivities in hydrocracking S_H ($\blacktriangle, \triangle$), isomerization plus dehydrocyclization S_{ID} (\blacklozenge, \lozenge), and aromatizations S_A ($\blacktriangledown, \triangledown$). Evolution with the overall conversion on catalyst VI-6. Black and white dots correspond to two independent experiments.

TABLE 7

Selectivity in 1-5 and 1-6 Dehydrocyclization of C₇ Hydrocarbons. Comparison with the Probability of Statistical Dehydrocyclization

Reactant	Catalyst	S ₁₋₅	S ₁₋₆
<i>n</i> -Heptane	VI-1	81	12
	VI-6	58	42
	Prob ^a	60	40
3-Methylhexane	VI-1	88	12
	VI-6	72	28
	Prob ^a	75	25
2,4-Dimethylpentane	VI-1	99	1
	VI-6	95	5
	Prob ^a	100	0

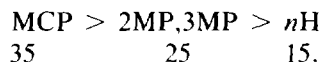
^a Probability of 1-5 + 1-6 dehydrocyclization.

In order to obtain more information on the relative selectivity towards 1-5 or 1-6 dehydrocyclization (Scheme 4), we compare the initial cyclization selectivities S₁₋₅ and S₁₋₆ on *n*-heptane, 3MH, and 2,4-dimethylpentane (Table 7). At low conversion, we can neglect in a first approximation the hydrogenolysis of the rings, which is justified as the rate of hydrogenolysis of C₆ rings is much lower than C₅ rings (2).

Whatever the hydrocarbon, the cyclization probability is statistical on the catalyst calcined at 900°C (VI-6), whereas the 1-5 cyclization probability is clearly higher on the uncalcined sample (VI-1).

We consider also the initial distribution in hydrocracking. As with 2MP, demethyl-

ation is largely the main process. Among the hexanes, however, the main product is MCP, which is somewhat unexpected, as MCP cannot be obtained in one single step but through dehydrocyclization followed by demethylation of the ring. This product distribution remains unchanged among the different catalysts:



5. XPS Studies

X-ray photoelectron spectroscopy studies were performed in order to investigate the electronic state of palladium. Binding energies are referenced to the Al 2*p* line at 74.9 eV. Pd 3*d*_{5/2} core-level peaks occur at 335.5 ± 0.3 eV, after an *in situ* reduction, whatever the catalyst (Table 8). Palladium is thus mainly in a metallic state. On a catalyst preoxidized in air *in situ* at 400°C, the Pd 3*d*_{5/2} core level shifts fully to 337.6 eV, a value which is 1.8 eV higher than metallic palladium obtained by consecutive reduction of the sample (Fig. 7). Such a shift can be attributed to a complete surface oxidation of palladium or even to PdO formation (31, 32).

The surface ratio Pd/Al decreases with calcination temperature (Table 8). This is in

TABLE 8

XPS Results on Pd/Al₂O₃ Catalysts
(Reference Al 2*p* at 74.9 eV)

Catalyst	E _B (Pd 3 <i>d</i> _{5/2}) (eV)	Pd 3 <i>d</i> /Al 2 <i>p</i> (10 ⁻²)	Cl 2 <i>p</i> /Al 2 <i>p</i> (10 ⁻²)
I-1	335.6	0.73	—
VI-1	335.2	13.	4
VI-2	335.2	9.3	2
VI-3	335.5	6.0	nd ^a
VI-4	335.7	4.4	nd ^a
VI-6	335.4	3.2	traces

^a Nondetermined.

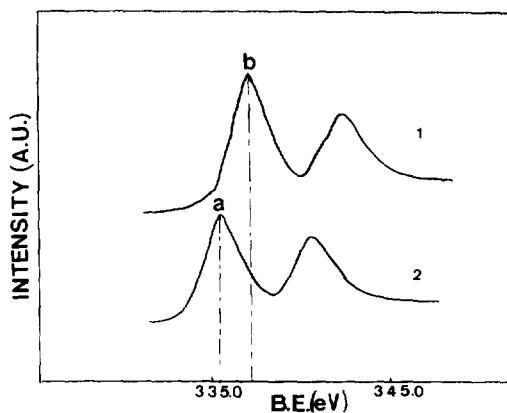


FIG. 7. Pd 3*d* lines on catalyst VI-3: (1) after 4 h calcination in air at 400°C followed by (2) 1 h reduction by H₂ at 300°C.

correlation with the reported catalytic activities except for the uncalcined sample. Chlorine surface content decreases also with calcination temperature. In addition we have noted an iron segregation at 900°C calcination, an effect which has been reported elsewhere by Auger spectroscopy on Pd/Al₂O₃ catalysts (33).

The nature of the palladium-support interface was investigated on catalyst VI-2 by comparing the shapes of Pd 3d core-level spectra both on the as-mounted sample, obtained by the passivation process of the reduced catalyst described in the experimental part, and on the same sample which is further *in situ* reduced. The 3d shapes are fitted with an analysis program (34) including:

—A Doniach-Sunjic-type contribution represented by an asymmetric Lorentzian function (35). Parameters for palladium used in the fit were published elsewhere (36).

—An experimental broadening given by a Gaussian-type function (1.1 eV).

—The inelastic processes and background contributions taken into account by a Shirley-type function.

Whereas the reduced catalyst is well fitted by a unique metallic contribution, a second contribution must clearly be added to the as-mounted sample at 1.8 eV on the high energy side of the metallic contribution (Fig. 8). This contribution, which is assumed to be of symmetric shape, represents 6% ± 2% of the total Pd 3d core level area. In addition, the metallic binding energy is lowered by 0.4 eV after an *in situ* reduction. This trend is systematically observed and is in good agreement with reported data (37).

DISCUSSION

1. Mechanisms

First we go into more detail on the reforming mechanisms encountered in this study. As firmly established by several groups these reactions involve some well-known intermediates in our experimental conditions.

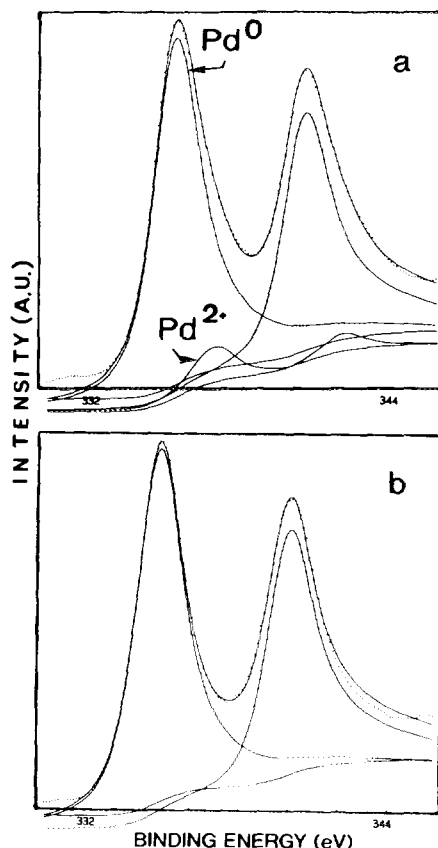


Fig. 8. XPS Pd 3d shape analysis of the sample VI-2: (a) as mounted followed by (b) reduction at 300°C.

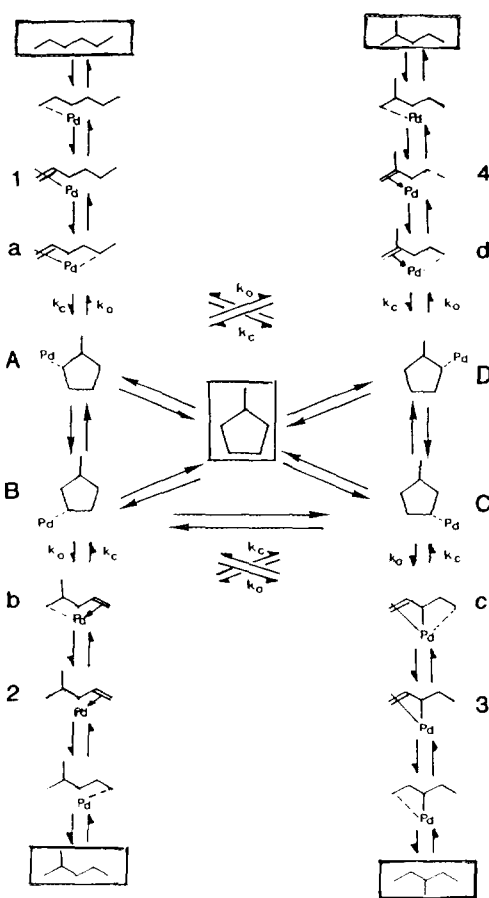
The *dehydrocyclization* and the reverse reaction of *cyclic hydrogenolysis mechanism* on Pd/Al₂O₃ occurs through bond insertion of a π olefin- σ alkyl 1,2-5 intermediate (5, 6). This step is well known in metathesis with palladium complexes (38), whereas the occurrence of π olefin complexes on palladium catalysts is well supported by early works on deuterium exchange (39). Paal and Tétényi (8), however, show that on platinum the product distribution in hexane isomerization and dehydrocyclization is strongly dependent on the hydrogen partial pressure. Despite the fact that there are not so many data on palladium, we have no reason to suspect a different behaviour. A low hydrogen pressure (or a high temperature) results in more dehydro-

generated intermediates. We believe, however, that at 300°C and under 1 atm hydrogen pressure the π olefin- σ alkyl 1,2-5 complexes are the more probable intermediates.

We focus now on the selectivity pattern induced by such a process. From the product distribution of MCP hydrogenolysis we can outline two main points:

—The distribution is rather insensitive to the precursor salt, the calcination temperature or the metallic dispersion. These results are in good agreement with literature (13), whereas only the influence of the acidity and the nature of the support (40) are reported. The behaviour of palladium differs thereby from platinum, where the product distribution is highly sensitive to the metallic dispersion. The MCP hydrogenolysis is statistical on the small platinum particles, whereas the *n*-hexane formation is inhibited on the large particles. Palladium exhibits also some inhibition towards *n*-hexane formation, but this behaviour is intermediate between the two extreme distributions obtained on platinum. —We cannot obtain a good agreement with a product distribution calculated from a statistical carbon-carbon bond rupture, excluding the exocyclic bond rupture (Distribution A in Table 2). Even if we consider the occurrence of a steric hindrance induced by an alkyl group on the adsorbed π olefin, as first proposed by Herington and Rideal in the aromatization on chromium oxides (41, 42) and again claimed on palladium (6), we cannot fit the experimental product distribution by the distribution B thus obtained or by some linear combination of distribution A and B. Furthermore, we can exclude isomer rearrangements controlled by the thermodynamics (Table 2) as hexane isomerization rate is much lower than MCP hydrogenolysis.

Taking into account these results, we depict in Scheme 5 a mechanism for both (i) methylcyclopentane hydrogenolysis and (ii) isomerization of hexanes through π olefin- σ alkyl 1,2-5 and σ alkyl intermediates. The π



SCHEME 5

olefin- σ alkyl 1,2-5 complexes a, b, c, and d are the precursor intermediates for the dehydrocyclization of hexanes. In the reverse reaction, the σ -alkyl adsorbed methylcyclopentane (A, B, C, D) intermediates give by direct cleavage of the carbon-carbon bond and subsequent hydrogen migration the π olefin- σ alkyl 1,2-5 complex. We assume that the methylcyclopentane is adsorbed on a secondary carbon of the ring only. By further statistical hydrogenolysis of the ring, we obtain the theoretical distribution C (Table 2) in close agreement with the experimental one. Furthermore, the invariability of activation energies with the product of hydrogenolysis supports also the hypothesis that the carbon-carbon rupture is nearly statistical.

The oriented formation of a σ -type adsorbed methylcyclopentane can be related to the electronic densities on each carbon of the ring. Hoffman (43) has shown that there is a high electronic density on the carbons α and β to the tertiary carbon and a very poor electronic density on the tertiary carbon itself (see Scheme 6 in Ref. (40b)). The palladium is an electron acceptor, possibly in the Pd^+ state, and thus promotes the methylcyclopentane adsorption on secondary carbons only (44). An alternative explanation can be the steric hindrance induced on a tertiary carbon by a metal-carbon σ bond.

Whatever the explanation, a similar behaviour is reported in an early work by Muller and Gault (5b): Dehydrocyclization of the 2,2,3-trimethylpentane occurs to a very high rate, whereas the 2,2,4-trimethylpentane cyclization exhibits a negligible activity. In this last molecule, the intermediate cyclopentane must be adsorbed on a tertiary carbon atom. Additionally, this mechanism is also in good agreement with product distribution reported from ethyl (7) and propyl (45) cyclopentane hydrogenolysis on $\text{Pd}/\text{Al}_2\text{O}_3$.

Compared with the distribution C, the small enhancement in 3-methylpentane to the detriment of 2-methylpentane can be explained in our scheme by the higher stability of intermediate species c compared to d.

We add a second assumption to this mechanism. The slow step of the isomerization process is the dehydrocyclization step k_c . This can be ascertained in our results by:

- the relative proportion of 3-methylpentane and *n*-hexane which are identical both in MCP hydrogenolysis and 2MP isomerization;
- the nonscrambling of the ^{13}C isotopic label;
- the higher rate of MCP hydrogenolysis compared with 2MP isomerization.

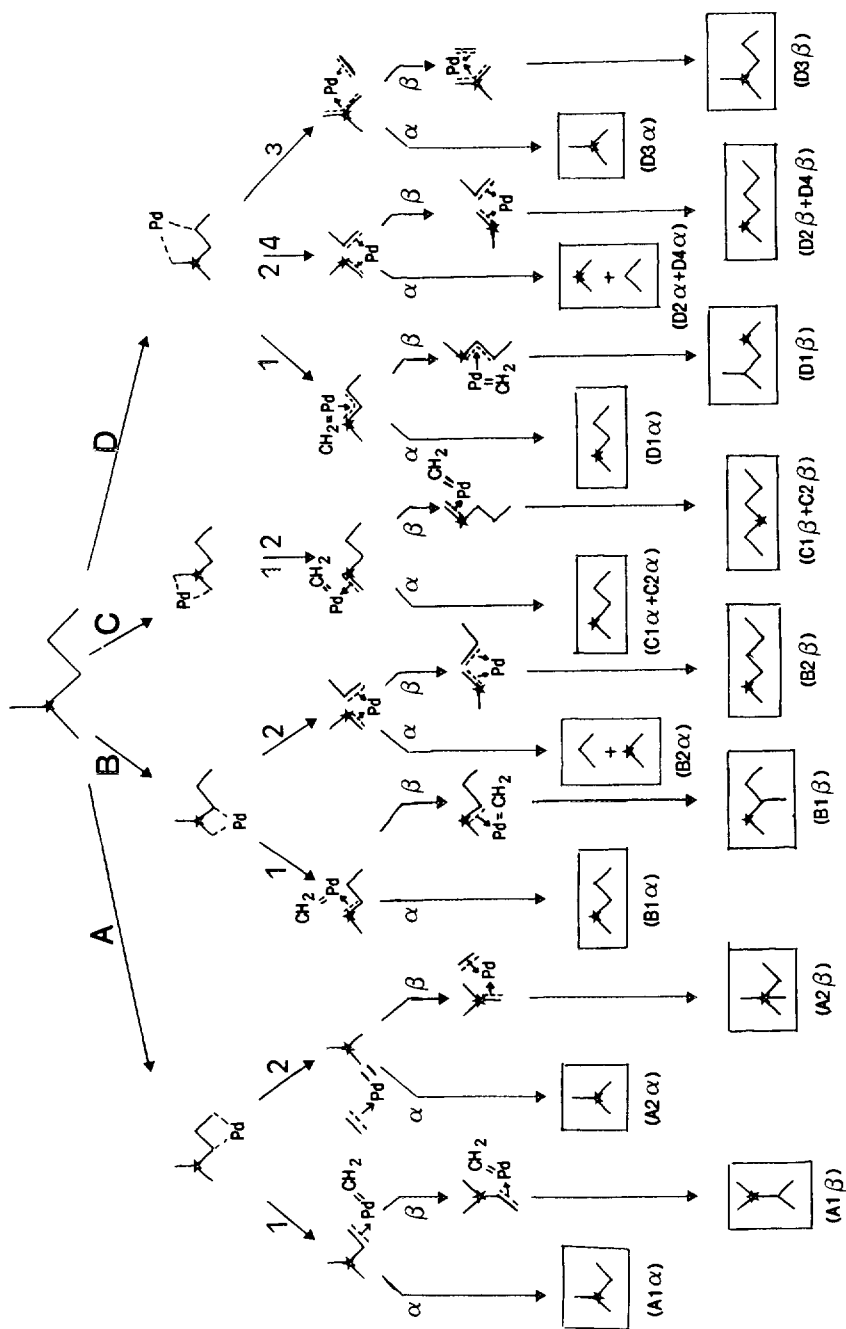
Apparent activation energies for both reactions are similar and range between 55 and 65 kcal/mol. Del Angel *et al.* (13) reported

slightly lower values (45 kcal/mol) for MCP hydrogenolysis. The reasons for this difference are not yet clear, but could be due to different hydrocarbon and hydrogen surface coverage expected with different experimental partial pressures. It has been shown that apparent activation energies are strongly dependent on these kinetic parameters (46).

Recently another mechanistic pathway has been claimed to explain the neopentane reactivity on $\text{Pd}/\text{Al}_2\text{O}_3$ catalysts (12). It includes the generation of Pd^{n+} sites, by occupation of vacant octahedral sites of the support. These sites are strong Lewis acid centers and thus induce, through a hydride abstraction, a carbenium ion mechanism. We can rule out this mechanism in the hexane isomerization, however, as the ^{13}C isotopic scrambling obtained through an acidic mechanism is formally identical to the bond shift mechanism, which is always minor in our present study (47, 48).

Apart from isomerization, however, the main reaction occurring on 2MP is the *demethylation* giving *n*-pentane and isopentane. Gault (2) proposed a mechanism that could explain both the demethylation and the bond shift isomerization. It occurs through a well-known metallacyclobutane intermediate followed by a hydrogenolysis giving a metallocarbene and an adsorbed π -olefin.










We propose to extend this mechanism by adding two further assumptions. First, we suppose that both metallacyclobutane and metallacyclopentane can be formed with an equal probability on palladium. The literature on the occurrence of metallacyclopentane is well provided in the organometallic chemistry of palladium (49). We exclude the formation of a metallacyclohexane as we believe that it is rapidly converted via 1-5 cyclization into an adsorbed cyclopentane (50). However, second, as for the cyclic isomerization of 2MP, we assume that the tertiary carbon cannot be involved into the metal-carbon bond of the metallacycle. The possible initial intermediates are then restricted to four (noted from A to D in



SCHEME 6

TABLE 9

Hydrocracking and Bond Shift Isomerization Product Distributions of ^{13}C -labelled 2MP on Pd/Al₂O₃ Catalysts

Products Catalyst									
Pathway (Scheme 6)	B2 + D2 + D4	A2 + D3	A1	B1 + C1 + D1 + C2	A2	A1	B2 + D2 + D4	C1 + C2	B1
I-1	2	3	36	59	4	ud	21	29	45
VI-1	3	3	41	53	6	ud	16	25	53
VII-1	5	4	38	53	2	19	14	14	51
Stat. dist.	37.5	19	6	37.5	8	8	17	50	17
ω (mean value)	0.1	0.2	6.2	1.5	0.4	~2	0.9	0.4	2.8

Scheme 6). For the sake of simplicity, only one palladium atom is represented in Scheme 6. This does not mean, however, that the hydrocarbon or its fragments are adsorbed on a single palladium atom, but more probably on an "ensemble."

The products of hydrogenolysis are the methylene (Path 1) or a substituted metallo-carbene (Path 2) and a π olefin or a metallacyclobutane. The alkyl-substituted metallo-carbenes Pd=CH—CHRR' are rapidly converted into a π olefin complex CH₂=CHRR'. The direct desorption (a) or the recombination only after the olefin rotation (b) gives the hydrocracked or the bond shift isomer products, respectively. The high selectivity towards demethylation (30–50%) instead of isomerization (<10%) can be explained by a barrier to the olefin rotation which is about 10–15 kcal/mol (2). We reported in Table 9 the experimental distribution in hydrocracking and bond shift isomerization which could be separately extracted when the ^{13}C label is used. These distributions are compared with a calculated one, taking into account an equal probability factor λ_{stat} for each pathway. We calculate then an actual probability factor ω according to Eq. (3). Mean values of ω are reported. These values exhibit only small variations with Pd/Al₂O₃ samples.

The hydrocracking pathways can be ranked in the decreasing order:

$$A1 > (B1 + C1 + C2 + D1) \\ \gg (A2 + D3), (B2 + D2 + D4),$$

whereas in bond shift isomerization only a partial distribution can be obtained as (i) autoisomerization (D1) cannot be determined with enough accuracy and (ii) 2,3-dimethylbutane (A1) is obtained in only one experiment. Nevertheless we obtain the following decreasing order:

$$B1 > A1 > (B2 + D2 + D4) \\ > A2, (C1 + C2).$$

Despite the partial and qualitative character of these results, we point out some similar trends:

—The pathway 1 of demethylation is predominant in both distributions. This can be explained by the high reactivity of the M=CH₂ metalcarbene, whereas the alkyl-substituted metalcarbenes can be rapidly converted into a more stable adsorbed π olefin as seen above.







—Among the initial metallacycles, the species A seems favoured. Steric reasons are probably at the origin of this stability.

Finally, another interesting point concerns the distribution of 3MP (Table 10).

—First the selectivity pattern in demethylation for two catalysts of different dispersions is modified. The metallacyclobutane formation according to our proposed mech-

TABLE 10

Hydrocracking and Bond Shift Isomerization Selectivity Pattern ω of ¹³C-labelled 3MP on Pd/Al₂O₃ Catalysts

Catalyst	Products					
						
I-1	0.08	3.3	1.3	—	3.7	0.3
VI-1	0.08	4.3	0.7	—	3.5	0.4

anism (scheme not represented here for 3MP) gives selectively *n*-pentane, whereas the metallacyclopentane formation gives both isopentane and *n*-pentane. Thus increasing selectivity towards *n*-pentane points out that the metallacyclobutane pathway is promoted on small particles. These results are in agreement with Coq and Figueras (51), who first reported a strong particle size effect on rhodium catalysts in the trimethylbutane demethylation. They explained it by a selective formation of metallacyclobutane to the detriment of metallacyclopentane on small particles.

—Second, we must underline the complete absence of 3MP autoisomerization from the 3-¹³C to the 2-¹³C species which can be obtained via some *n*β pathways (*n* ≥ 2). This is a strong indication of (i) the minor role played by the pathways *n* but (ii) this suggests also that an acidic mechanism can be ruled out as this autoisomerization process

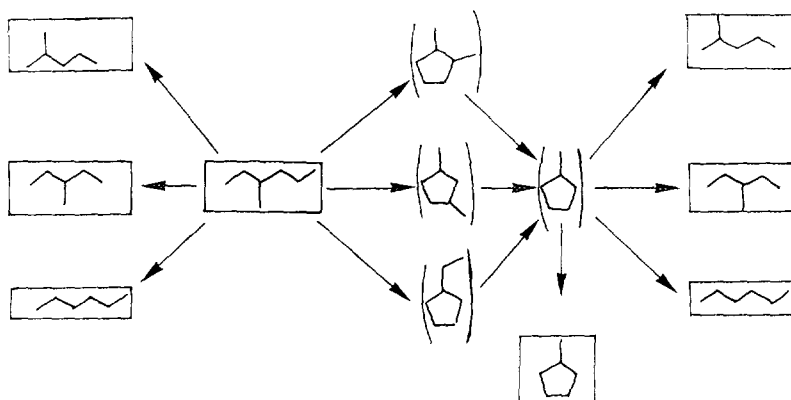
is the predominant pathway on purely acidic catalysts (48).

Considering the 3MH demethylation, however, an alternative pathway must be introduced as the main hexane product is the unexpected MCP. We think that this alternative pathway occurs through fast dehydrocyclization followed by demethylation of the exocyclic hydrocarbon chain (Scheme 7). The occurrence of this mechanism can be supported by the fact that

—the 1-5 dehydrocyclization rate is increased for longer hydrocarbon chain such as 3MH (2).

—the demethylation rate of ethylcyclopentane is very fast on palladium (7).

Using isotopic labelling, the aromatization mechanism was described to be analogous to the 2MP dehydrocyclization mechanism (Scheme 5). Instead of π olefin-σ alkyl 1,2-5 intermediates it involves π olefin-σ alkyl 1,2-6 intermediates first described by Herington and Rideal (41, 42). The other mechanism, occurring through 1,2,5 dehydrocyclization followed by ring enlargement was found to be negligible (7). Useful information is obtained, however, on the initial competing processes of 1,2,5 or 1,2,6 cyclization that govern the aromatization selectivity. The 1,2,5 versus 1,2,6 cyclization is equally probable on the calcined catalyst,



SCHEME 7

whereas the 1,2,5 cyclization is promoted on the uncalcined sample. This selectivity effect occurs whatever the branching degree of the hydrocarbon. This striking difference can be related to the nature of the palladium surface. Low index planes are developed from a high-temperature calcination (52) on which the effect of steric hindrance are minimized. Dehydrocyclization thus occurs indifferently through 1,2,5 or 1,2,6 intermediates. On the uncalcined sample, however, more surface defects are present. On such sites 1,2,5 cyclization is probably less strained than 1,2,6 cyclization if we consider an adsorption parallel to the palladium surface.

In conclusion we can state that on Pd/Al₂O₃ the initial aromatization selectivity of a given hydrocarbon is limited by the competitive 1-6 and 1-5 dehydrocyclizations and the statistical probability of 1-6 dehydrocyclization represents an upper limit to this selectivity.

2. Influence of Palladium Precursor Salt, Calcination Temperature, and Particle Size

These influences are generally small both on activity and selectivity. However, the catalysts prepared from the nitrate precursor salt exhibit a much lower activity. One explanation is the weak dispersion obtained on this catalyst due to the poor interaction between the metal and the support. The same singularity is observed elsewhere in a complete study of Pd/Al₂O₃ modified by rare earth addition (53). On the other catalysts, the interaction between metal and support is stronger and results in a better dispersion of the metallic phase.

Some indications on the nature of the metal-support interaction can be obtained from XPS. From lineshape analysis on an "as-mounted" sample, we could deduce that about 5–10% of palladium is not in a metallic state, but probably in an oxidized or oxychlorided form at the interface of the metal and the support. Assuming a hemispherical shape of the metallic particle and

that the nonmetallic species is localized along the particle-support interface, the proportion s of these sites related to the total number of surface sites can be expressed to a first approximation as

$$s = 1/(a \cdot r \cdot (L)), \quad (6)$$

where $a = 0.277$ nm is the metal-metal distance, r the mean diameter of the metallic particle, and L the mean atomic density of sites taken as 1.27×10^{15} atoms/cm². In our case with $r = 3.5$ nm we obtain $s = 8\%$, a value well in agreement with the experimental lineshape analysis. It can thus be concluded that, in a passivated form, the interface between support and metallic particle is oxidized and that the metal-support interaction is strong. In a similar way, there is reported from infrared spectroscopy of chemisorbed CO and EPR the occurrence of Pdⁿ⁺ ions which are assigned however to palladium ions in octahedral vacant sites of the support (54). After the reduction, the palladium at the interface is fully reduced. Furthermore, as the selectivity is not very sensitive to the palladium dispersion, and then to the metal-support interface, it seems thus doubtful, even if it could not be excluded, to attribute some special activity to the sites localized at the interface.

In conclusion we must outline the importance of palladium precursor salt on the generation of a metal-support interaction and thus on the catalytic activity. This interaction, however, does not modify the selectivity.

—The variation of activity with calcination temperature is included within one order of magnitude. The maximum between 200 and 400°C could be related to some oxide formation during the calcination, as evidenced by XPS, and a better wetting of the oxide or oxychloride phase with the support (55). The slight decrease in activity at higher calcination temperature could be explained by both metallic sintering and a loss of surface area of the support. Small changes in selectivity occur, however, with the calcina-

tion temperature. 3MH aromatization is noticeably increased at high calcination temperatures. We have seen above that this increase does not exceed the statistical probability of 1,2,6 cyclization and can probably be related to the topology of the palladium surface. We detect, however, by XPS a surface segregation of iron after the high-temperature calcination, whereas the overall iron content in alumina does not exceed 200 ppm, as checked by microanalysis. This may suggest an alternative explanation. It was claimed that Pd-Fe alloys inhibit hydrogenation reactions (33). Thus iron segregation or even alloy formation (not detected by XRD analysis) induced by high calcination temperature can strongly favour dehydrogenated products. The selectivity change would be then an impurity effect. Clearly additional work is needed to clarify this point.

We can evaluate a turnover frequency only on catalyst I-1 and II-2 as they exhibit a rather homogeneous particle distribution. From the activity A_i in a given reaction i , the turnover frequency ν_i is given by

$$\nu_i = (A_i \cdot N \cdot n_m \cdot d_s) / (a \cdot L), \quad (7)$$

where a is a geometric factor taken as 5 if we assume a cubic shape of the particle of edge d_s (nm), n_m is the palladium density, and L is given above. With these values, ν_i expressed in h⁻¹ takes the form

$$\nu_i = 0.4 \cdot d_s \cdot A_i. \quad (8)$$

In methylcyclopentane hydrogenolysis, turnover frequencies (TOF) range between 50 and 100 h⁻¹. For comparison with already published data, these values mean TOF of 6 to 12 h⁻¹ at 280°C, with an activation energy of 65 kcal/mol, as reported above. This compares fairly well with values of 3 to 5 h⁻¹ reported at this temperature by Del Angel *et al.* (13).

In 2MP isomerization, TOF values are 5–10 h⁻¹ at 300°C.

—The only effect of particle size that we note clearly is an increase at high dispersion

in the cyclic mechanism to the detriment of demethylation. We note also that this increase is mainly due to an increase in the methylcyclopentane content. Two comments must be added:

(1) First this behaviour on palladium resembles the behaviour of platinum, where the cyclic mechanism is also promoted at high dispersion but to the detriment of the bond shift. Unlike platinum, however, the change in particle size does not induce a change in MCP selectivity from a nonselective to a selective carbon bond rupture (2).

(2) As has been seen above, the demethylation and the main isomerization on palladium involve essentially different intermediate species, i.e. π olefin- σ alkyl 1,2-5 and metallacycle intermediates for the cyclic mechanism and the demethylation, respectively.

This last remark allows us to rule out any geometrical effect in this mechanistic change. One explanation could be the occurrence of additional reactions at the metal-support interface, but for the reasons seen above this seems unlikely. We therefore think that modifications of electronic properties in small particles induced by a smaller coordination of atoms can best explain this change in selectivity. Hydrogen and hydrocarbon adsorption capacity are changed on these small particles. The stability of the dehydrogenated intermediate complex is then shifted. As demethylation involves the formation of highly dehydrogenated π olefin and metallocarbene intermediates (Scheme 6), the cyclization pathway will be preferred as giving a less dehydrogenated species which can be more easily desorbed. Moreover the direct desorption of the σ -adsorbed methylcyclopentane will be preferred to a further hydrogenolysis of the ring (Scheme 3). In a similar way, it has been reported that on small palladium particles the turnover number in the hydrogenation of highly dehydrogenated olefins such as butyne, butadiene, or iso-

prene is strongly decreased with increased dispersion (56).

CONCLUSIONS

We may summarize the main results of this work as follows.

—The use of different reforming reactions in the C₆–C₇ range and of ¹³C isotopic labelling allows us to define more accurately the mechanistic pathways on Pd/Al₂O₃ catalysts.

—The constant selectivity in MCP hydrogenolysis can be best explained by a selective adsorption on the secondary carbon atom. We can then satisfactorily explain both the selectivity in MCP hydrogenolysis and 2MP isomerization.

—The demethylation, the most intense hydrocracking reaction, and the bond shift isomerization are parallel processes including metallacyclobutane and metallacyclopentane intermediates.

—For hydrocarbons with a long chain, however, another hydrocracking process occurs through dehydrocyclization followed by hydrogenolysis of the exocyclic hydrocarbon chain.

—The initial aromatization selectivity, occurring through π olefin- σ alkyl 1,2-6 intermediates, is limited by competitive 1-5 and 1-6 dehydrocyclizations.

—The influence of the calcination temperature is weak on the activity, whereas the aromatization selectivity is noticeably increased at high calcination temperature.

—The selectivity towards 2MP dehydrocyclization increases slightly to the detriment of demethylation on small particles. This small size effect, similar to the behaviour of platinum, is best explained by the higher stability of highly dehydrogenated intermediates.

—The influence of the palladium precursor salt on activity is large. The nitrate precursor catalysts exhibit a poor activity compared to the chloride or the acetylacetonate precursor catalysts. This last point, however, requires further investigation. We can

thus address the following questions, among others: What is the true nature of metal–support interaction?; what is the role of the metal–support interface and what is the importance of support acidity, in the light of recent work performed on zeolite as support (40)?

ACKNOWLEDGMENTS

The contributions of G. Ehret for TEM examinations and M. Bacri for BET analysis are greatly appreciated. Many thanks are due to Dr. J. P. Boitiaux (I.F.P.) for the gift of a catalyst. We also acknowledge Dr. F. Garin, L. Hilaire, M. Pfeffer, V. Pitchon, and R. Touroude for many helpful discussions.

REFERENCES

1. Franck, J. P., in "Catalyse par les Métaux," Vol. 401, Editions du CNRS, Paris, 1984.
2. Gault, F. G., in "Advances in Catalysis" (D. D. Eley, H. Pines, and P. B. Weisz, Eds.), Vol. 30, p. 1, Academic Press, New York, 1981.
3. (a) Maire, G., and Garin, F., in "Catalysis, Science and Technology" (J. R. Anderson and M. Boudart, Eds.), Vol. 6, p. 162, Springer-Verlag, Berlin, 1988; (b) *J. Mol. Catal.* **48**, 99 (1988); (c) *Acc. Chem. Res.* **122**, 100 (1989).
4. Anderson, J. R., and Avery, N. R., *J. Catal.* **5**, 446 (1966).
5. Sheppard, L. E., and Rooney, J. J., *J. Catal.* **3**, 129 (1964); (b) Muller, J. M., and Gault, F. G. in "Proceedings, 4th International Congress on Catalysis, Moscow, 1968" (B. A. Kazansky, Ed.), Adler, New York, 1968.
6. Hajek, M., Corolleur, S., Corolleur, C., Maure, G., O'Conneide, A., and Gault, F. G., *J. Chim. Phys.* **71**, 1329 (1974).
7. Chillès, J. F., Thesis, Université Louis Pasteur, Strasbourg, France, 1980.
8. (a) Paal, Z., and Tétényi, P., *Appl. Catal.* **1**, 9 (1981); (b) *React. Kinet. Catal. Lett.* **12**, 131 (1979); (c) Paál, Z., *Catalysis* **5**, 80 (1982).
9. Karpinski, Z., *Nouv. J. Chim.* **4**, 561 (1980).
10. Juszyk, W., Karpinski, Z., Pielaszek, J., Ratajczykowa, I., and Stanasiuk, Z., in "Proceedings, 9th International Congress on Catalysis, Calgary, 1988" (M. J. Phillips and M. Ternan, Eds.), p. 1238, Chem. Institute of Canada, Ottawa, 1988.
11. Juszyk, W., and Karpinski, Z., *J. Catal.* **117**, 519 (1989).
12. Juszyk, W., Karpinski, Z., Ratajczykowa, I., Stanasiuk, Z., Zielinski, J., Shen, L. L., and Sachtler, W. M. H., *J. Catal.* **120**, 68 (1989).
13. Del Angel, G. A., Coq, B., Ferrat, G., and Figueras, F., *Surf. Sci.* **156**, 943 (1985).
14. Karpinski, Z., Juszyk, W., and Stachurski, J., *J. Chem. Soc. Faraday Trans. 1* **81**, 1454 (1985).

15. O' Cinneide, A., and Gault, F. G., *J. Catal.* **37**, 311 (1975).
16. Karpinski, Z., *J. Catal.* **77**, 118 (1982).
17. Del Angel, G. A., Coq, B., and Figueras, F., *J. Catal.* **95**, 167 (1985).
18. Boitiaux, J. P., Cosyns, J., and Vasudevan, S., in "Proceedings, 3rd International Symposium on the Scientific Bases for the Preparation of Heterogeneous Catalysts," p. 123. Elsevier, Amsterdam, 1982.
19. Garin, F., and Gault, F. G., *J. Am. Chem. Soc.* **97**, 4466 (1975).
20. Dartigues, J. M., Chambellan, A., and Gault, F. G., *J. Am. Chem. Soc.* **98**, 856 (1976).
21. Dalmai-Imelik, G., Leclercq, C., and Mutin, I., *J. Microsc.* **20**, 123 (1974).
22. Antonin, G. A., Moraweck, B., Renouprez, A. J., Dalmai-Imelik, G., and Imelik, B., *J. Chim. Phys.* **3**, 532 (1972).
23. Whyte, T. E., Jr., *Catal. Rev.* **8**, 117 (1974).
24. Van Hardeveld, R., and van Montfoort, A., *Surf. Sci.* **4**, 396 (1966).
25. Farbotko, M., Kili, K., Le Normand, F., and Touroude, R., unpublished results.
26. Le Normand, F., Hilaire, L., Kili, K., Krill, G., and Maire, G., *J. Phys. Chem.* **92**, 2561 (1988).
27. Stull, D. R., Westrum, E. F., Jr., and Sinke, G. C., "The Chemical Thermodynamics of Organic Compounds," p. 349. Wiley, New York, 1969.
28. Leclercq, G., Leclercq, L., and Maurel, R., *J. Catal.* **50**, 87 (1977).
29. Chakroun, A., Thesis, Université Louis Pasteur, Strasbourg, France, 1983.
30. Boutonnet, M., Thesis, Université Louis Pasteur, Strasbourg, France, 1980.
31. Légaré, P., Hilaire, L., Maire, G., Krill, G., and Amamou, A., *Surf. Sci.* **107**, 533 (1981).
32. Kim, K., Gossmann, A., and Winograd, N., *Anal. Chem.* **46**, 197 (1974).
33. Bhasin, M. M., *J. Catal.* **38**, 218 (1975).
34. Romeo, M., Légaré, P., and Majerus, J., submitted for publication.
35. Doniach, S., and Sunjic, M., *J. Phys. C: Solid State Phys.* **3**, 285 (1969).
36. Hufner, S., and Wertheim, G. K., *Phys. Rev. B* **11**, 678 (1975).
37. Noack, K., and Schlogl, R., *Catal. Lett.* **4**, 145 (1990).
38. (a) Wilker, C. W., and Hoffmann, R., *J. Am. Chem. Soc.* **105**, 5285 (1983); (b) Berke, H., and Hoffmann, R., *J. Am. Chem. Soc.* **100**, 7224 (1978).
39. (a) Gault, F. G., Rooney, J. J., and Kembal, C., *J. Catal.* **1**, 225 (1962); (b) Rooney, J. J., *J. Catal.* **2**, 53 (1963).
40. (a) Hohmeyer, S. T., Karpinski, Z., and Sachtler, W. M. H., *J. Catal.* **123**, 60 (1990); (b) Le Normand, F., Barrault, J., Breault, R., Hilaire, L., and Kiennemann, A., *J. Phys. Chem.* **95**, 257 (1991).
41. Herington, E. F. G., and Rideal, E., *Proc. R. Soc. London Ser. A* **104**, 434 (1945).
42. Herington, E. F. G., and Rideal, E., *Proc. R. Soc. London Ser. A* **104**, 447 (1945).
43. Hoffmann, R., *J. Chem. Phys.* **39**, 1399 (1963).
44. Tolbert, M. A., Mandich, M. L., Halle, L. F., and Beauchamp, J. L., *J. Am. Chem. Soc.* **108**, 5675 (1986).
45. Cadieu, M. C., Thesis, Université Louis Pasteur, Strasbourg, France, 1987.
46. Frennel, A., in "Hydrogen Effects in Catalysis" (Z. Paál and G. Menon, Eds.), Dekker, Amsterdam, 1988.
47. Le Normand, F., Fajula, F., and Sommer, J., *Nouv. J. Chim.* **6**, 411 (1982).
48. Le Normand, F., Fajula, F., and Sommer, J., *Nouv. J. Chim.* **6**, 417 (1982).
49. Diversi, P., Ingrosso, G., Lucherini, A., and Murtas, S., *J. Chem. Soc. Dalton Trans.*, 1633, 1980.
50. Clarke, J. K. A., Finlayson, O. E., and Rooney, J. J., *J. Chem. Soc. Faraday Trans. 1* **80**, 191 (1984).
51. Coq, B., and Figueras, F., *J. Mol. Catal.* **55**, 34 (1989).
52. Gao, S., and Schmidt, L. D., *J. Catal.* **115**, 356 (1989).
53. Kili, K., and Le Normand, F., submitted for publication.
54. Karpinski, Z., *Catal. Lett.* **5**, 197 (1990).
55. Ruckenstein, E., and Chen, J. E., *J. Catal.* **70**, 233 (1981).
56. Vasudevan, S., Thesis, Institut Français du Pétrole, 1984.